Int. J. Adv. Appl. Math. and Mech. 6(4) (2019) 1 – 13 (ISSN: 2347-2529)

Journal homepage: www.ijaamm.com

IJAAMM

International Journal of Advances in Applied Mathematics and Mechanics

Modeling traffic flow on Multi-Lane road: Effects of lane-change manoeuvres due to an off-ramp

Research Article

William Kuria Ndungu[a,*], **Mark E. M. Kimathi**[b], **David Mwangi Theuri**[a]

[a] *Department of Pure and Applied Mathematics, Jomo Kenyatta University of Agriculture and Technology, Juja,62000-00200, Nairobi, Kenya*

[b] *Department of Mathematics, Statistics and Actuarial Sciences, Machakos University, Machakos,136-90100, Machakos, Kenya*

Received 14 February 2019; accepted (in revised version) 21 May 2019

Abstract: In this paper, a macroscopic multi-lane traffic flow model of Aw-Rascle type is outlined. Finite volume method (Godunov scheme) is used to solve the numerical model equations for each lane while Euler's method was used for the source term. We simulate traffic congestion near an off-ramp in a highway with three traffic lanes. Results of the traffic simulations in the vicinity of an off-ramp is presented inform of graphs and space-time plots. The results show that vehicle lane-change manoeuvre near the off-ramp lead to traffic congestion on the lane next to the off-ramp as compared to the other lanes, especially during rush hours. Thus vehicular lane change manoeuvres are crucial elements of traffic disturbance near bottlenecks. These results provide important insight into improving the road network design and safety management strategies especially when constructing new highways.

MSC: 35LXX • 76LXX

Keywords: Traffic congestion • Off-ramp • Finite volume method • Source term • Lane-change manoeuvre

1. Introduction

In our modern and upcoming urban towns, transportation of goods and passengers have become a major issue of concern. This is due to vehicular traffic congestion experienced in our roads network caused by traffic breakdown in an initially free flowing traffic near the bottlenecks such as on and off-ramps, Kerner [1]. At off-ramps, the exiting vehicles must change lanes to the outside lane of the highway to access the shoulder lane. This increased traffic density on the outside lane and possible decerelation of exiting traffic is likely to force the express motorway vehicles in the outer lane to change lanes to the inner lanes to avoid exiting traffic, Kondli and Elefteriadon [12]. These interaction of vehicles while making lanes change cause traffic congestion upstream of the off-ramps and adversely affect the available road capacity of expressways at these sections. Thus, even those vehicles on expressway experience long delays due to this congestion. Recent studies on traffic management have shown that lane-changing manoeuvres contribute to traffic flow disturbance on multi-lane freeways especially near the off-ramps Wei [13]. Generally vehicle lane-change can be classified as either mandatory or discretionary according to driving incentives. That is, mandatory lane-change occurs mostly at off-ramp or lane drop where vehicles are forced to change to a fixed target lane and lead to traffic breakdown due to the increased traffic demand on this road section. On the other hand discretionally lane-changing is conducted when the drivers perceive that driving conditions in the target lane are better. However, both

* Corresponding author.

E-mail address(es): willykuria@yahoo.com (William Kuria Ndungu), memkimathi@gmail.com (Mark E. M. Kimathi), dtheuri@gmail.com (David Mwangi Theuri).

lane-change sometime can be performed one after the other, especially when an aggressive driver decide to overtake a heavy vehicle infront first before performing mandatory lane-change to the off-ramp. Ahmed [7] used a random utility theory in lane changing behavior modeling and defined a lane changing choice as a sequence of decision to make lane change, choice of the lane and then look for an acceptable space gap to decide the way forward. Otherwise, for a vehicle to attempt any lane change under condition of traffic congestion it needs the co-operation from at least one of the following vehicle in the target lane. Amin and Banks [11] showed that, just upstream of an off-ramp, the fraction of flow on the outside lane is expected to be higher compared to an outside lane on a normal continuous stretch of motor way. Klar and Wegener [6] derived macroscopic traffic model equations by considering a highway with N-lanes and involved vehicle interactions when changing lanes. Earlier traffic flow theories and models failed to explain the traffic breakdown at the highway bottleneck as observed in real measured traffic data because of missing the discontinuous character of probability of passing, Kerner [1]. Thus the need to develop a macroscopic traffic flow model of Aw-Rascle type which is able to explain the co-existence of free flow, synchronized flow and wide moving jams as observed in real measured traffic data. This model explicitly takes into account the dynamics of traffic at off-ramps by modeling the lane changing manoeuvres within this region.

2. Mathematical model

2.1. The Kinetic Traffic Multi-lane Flow Model

The kinetic traffic flow model is described by use of the distribution functions of velocity of vehicles in traffic flow. We consider a highway with N lanes numbered by $\alpha = 1, ..., N$. Letting $f_\alpha(x, v)$ denote a single car distribution function which describes the number of cars at x with velocity v on lane α. If $F_\alpha(x, v)$ denote the probability distribution in v of cars at x i.e. $f_\alpha(x, v) = \rho_\alpha(x) F_\alpha(x, v)$, $F_\alpha^+(v_+; h, v, x)$ denote the probability distribution in v_+ of the leading cars at distance h for cars at x with velocity v, and $Q_\alpha(h; v, x)$ denote the probability distribution of leading cars in h for a car at x with velocity v, then;

$$f_\alpha(x, v, h, v_+) = F_\alpha^+(v_+; h, v, x)\, Q_\alpha(h; v, x)\, f_\alpha(x, v) \tag{1}$$

Assuming the leading vehicles are distributed according to the probability $F_\alpha(x, v)$ at $x + h$ i.e $F_\alpha^+(v_+; h, v, x) = F_\alpha(x + h, v_+)$ and $Q_\alpha(h; v, x) = q_\alpha\left(h; v, f_\alpha(x, v)\right)$ then

$$f_\alpha(x, v, h, v_+) \sim q_\alpha\left(h; v, f_\alpha(x, v)\right) F_\alpha(x + h, v_+)\, f_\alpha(x, v) \tag{2}$$

Here the kinetic equation for the distribution functions $\left(f_1, ..., f_N\right)$ on N lanes is obtained by finding the kinetic interaction operators, Klar and Wegener [6] i.e the Gain (G) and Loss (L) operators:

$$\begin{aligned}
&\partial_t f_\alpha + v\partial_x f_\alpha = C_\alpha^+\left(f_1, ..., f_N\right) = \left(G_B^+ - L_B^+\right)\left(f_{\alpha-1}, f_\alpha, f_{\alpha+1}\right) \\
&+ \left(G_A^+ - L_A^+\right)\left(f_\alpha\right) + \left[G_R^+\left(f_\alpha, f_{\alpha+1}, f_{\alpha+2}\right) - L_R^+\left(f_\alpha, f_{\alpha+1}\right)\right] \\
&+ \left[G_L^+\left(f_{\alpha-1}, f_\alpha\right) - L_L^+\left(f_{\alpha-1}, f_\alpha, f_{\alpha+1}\right)\right]
\end{aligned} \tag{3}$$

Taking $\rho_\alpha = \int_0^w f_\alpha(x, v)\, dv$, $f_\alpha = \rho_\alpha F_\alpha$ and $q_X\left(v, f_\alpha\right) = q\left(H_X(v), v, f_\alpha\right)$ where $H_X(v)$; $X = B, A$ is the threshold for braking and acceleration respectively. The left hand side of the partial differential equation (3) describes the continuous dynamics of the phase-space density (PSD) due to the motions of traffic flow while the right hand side describes the discontinuous changes of this function due to lane-changing, acceleration and deceleration. Defining probability P_Y, $Y = L, R$ for a lane change to either left (L) or right (R) and using the convention $P_R\left(v, f_{N+1}\right) = P_L\left(v, f_0\right) = 0$, then the gain and loss terms in equation (3) can be approximated as follows, taking lane α as the considered lane:

Remark 2.1.
In this study drivers are bound to the left-hand side rule by which it is mandatory for slow moving vehicles to keep left lane unless overtaking. The following Fig. 1 shows the multi-lane highway under consideration in our traffic flow modeling. The arrows indicate the gain and loss interaction terms due to vehicle changing lanes to their target lanes.

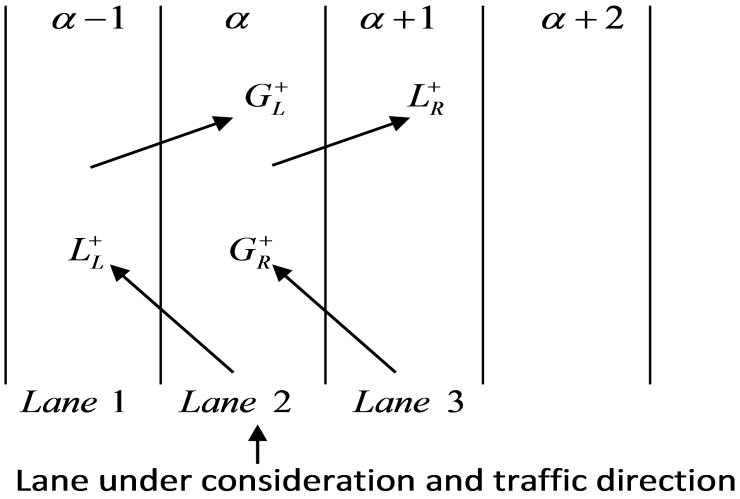

Fig. 1. Section of the multi-lane highway showing the kinetic traffic interaction operators due to lane-changing manoeuvres.

Gain and Loss Due to Lane Changing to the Right

A vehicle will change lane to the right if the braking line is reached and a lane change is possible with a probability P_R, resulting to the following vehicle interactions:
(a) *Gain term from the right (G_R^+) defined as;*

$$G_R^+\left(f_\alpha, f_{\alpha+1}, f_{\alpha+2}\right) = \int_{\hat{v}_- > v} P_L\left(v,\rho_\alpha\right)\left[1-P_R\left(\hat{v}_-,\rho_{\alpha+2}\right)\right]|v-\hat{v}_-|q_B\left(\hat{v}_-,\rho_{\alpha+1}\right) \times \rho_{\alpha+1}\delta u_{\alpha+1}^-\left(\hat{v}_-\right)\delta u_{\alpha+1}\left(v\right)d\hat{v}_- \tag{4}$$

(b) *Loss term to the right* $\left(L_R^+\right)$ *defined as:*

$$L_R^+\left(f_\alpha, f_{\alpha+1}\right) = \int_{v>\hat{v}_+} P_R\left(v, f_{\alpha+1}\left(x,v\right)\right)|v-\hat{v}_+|q_B\left(H_B\left(v\right), f_\alpha\left(x,v\right)\right)\rho_\alpha\delta u_\alpha\left(v\right)\delta u_\alpha^+\left(\hat{v}_+\right)d\hat{v}_+$$

$$= \int_{v>\hat{v}_+} P_R\left(v,\rho_{\alpha+1}\right)|v-\hat{v}_+|q_B\left(H_B\left(v\right),\rho_\alpha\right)\rho_\alpha\delta u_\alpha\left(v\right)\delta u_\alpha^+\left(\hat{v}_+\right)d\hat{v}_+ \tag{5}$$

Gain and Loss Due to Lane Changing to the Left

A vehicle will change lane to the left if it reaches the braking line and is not able to overtake using the right lane. This yields the vehicle interactions defined below:
(a) *Gain term from the left lane* (G_L^+) *defined as*:

$$G_L^+\left(f_{\alpha-1}, f_\alpha\right) = \int_{v>\hat{v}_+} P_R\left(v, f_\alpha\left(x,v\right)\right)|v-\hat{v}_+|q_B\left(H_B\left(v\right), f_{\alpha-1}\left(x,v\right)\right)\rho_{\alpha-1}\delta u_{\alpha-1}\left(v\right)\delta u_{\alpha-1}^+\left(\hat{v}_+\right)d\hat{v}_+$$

$$= \int_{v>\hat{v}_+} P_R\left(v,\rho_\alpha\right)|v-\hat{v}_+|q_B\left(H_B\left(v\right),\rho_{\alpha-1}\right)\rho_{\alpha-1}\delta u_{\alpha-1}\left(v\right)\delta u_{\alpha-1}^+\left(\hat{v}_+\right)d\hat{v}_+ \tag{6}$$

(b) *Loss term to the left* (L_L^+) *defined as*:

$$L_L^+\left(f_{\alpha-1}, f_\alpha, f_{\alpha+1}\right) = \int_{\hat{v}_- > v} P_L\left(v,\rho_{\alpha-1}\right)\left[1-P_R\left(\hat{v}_-,\rho_{\alpha+1}\right)\right]|v-\hat{v}_-| \times q_B\left(\hat{v}_-,\rho_\alpha\right)\rho_\alpha\delta u_\alpha^-\left(\hat{v}_-\right)\delta u_\alpha\left(v\right)d\hat{v}_- \tag{7}$$

Gain or Loss Due to Vehicles Acceleration

A vehicle will accelerate if the acceleration line is reached. Therefore:
(*a*) *Gain term from acceleration* (G_A^+) *is defined as:*

$$G_A^+(f_\alpha) = \iint_{\hat{v}<\hat{v}_+} |\hat{v}-\hat{v}_+|\sigma_A(v,\hat{v})\, q_A\left(H_A(\hat{v}), f_\alpha(x,\hat{v})\right)\rho\delta u_\alpha(\hat{v})\,\delta u_\alpha^+(\hat{v}_+)\,d\hat{v}d\hat{v}_+$$

$$= \int\int_{\hat{v}<\hat{v}_+} |\hat{v}-\hat{v}_+|\sigma_A(v,\hat{v}_+)\, q_A\left(H_A(\hat{v}), \rho_\alpha\right)\rho_\alpha\delta u_\alpha(\hat{v})\,\delta u_\alpha^+(\hat{v}_+)\,d\hat{v}d\hat{v}_+ \tag{8}$$

(*b*) *Loss term from acceleration* (L_A^+) *is defined as*:

$$L_A^+(f_\alpha) = \int_{v<\hat{v}_+} |v-\hat{v}_+| q_A\left(H_A(v), f_\alpha(x,v)\right)\rho_\alpha\delta u_\alpha(v)\,\delta u_\alpha^+(\hat{v}_+)\,d\hat{v}_+$$

$$= \int_{v<\hat{v}_+} |v-\hat{v}_+| q_A\left(H_A(v), f_\alpha(x,v)\right)\rho_\alpha\delta u_\alpha(v)\,\delta u_\alpha^+(\hat{v}_+)\,d\hat{v}_+ \tag{9}$$

Gain or Loss Due to Vehicles Deceleration

A vehicle will brake if it reaches the braking line and the driver is not able to change to the right or left lane. Therefore:
(*a*) *Gain term from braking interaction* (G_B^+) *is defined as*:

$$G_B^+(f_{\alpha-1}, f_\alpha, f_{\alpha+1})$$

$$= \iint_{\hat{v}>\hat{v}_+} P_B(\hat{v},\hat{v}_+,\rho_{\alpha-1},\rho_{\alpha+1})|\hat{v}-\hat{v}_+|\sigma_B(v,\hat{v})$$

$$\times q_B\left(H_B(\hat{v}),\rho_\alpha\right)\rho_\alpha\delta u_\alpha(\hat{v})\,\delta u_\alpha^+(\hat{v}_+)\,d\hat{v}d\hat{v}_+ \tag{10}$$

(*b*) *Loss term from braking interaction* (L_B^+) *is defined as*:

$$L_B^+(f_{\alpha-1}, f_\alpha, f_{\alpha+1})$$

$$= \int_{v>\hat{v}_+} P_B(v,\hat{v}_+,\rho_{\alpha-1},\rho_{\alpha+1})|v-\hat{v}_+| q_B\left(H_B(v),\rho_\alpha\right)\rho_\alpha\delta u_\alpha(v)\,\delta u_\alpha^+(\hat{v}_+)\,d\hat{v}_+ \tag{11}$$

2.2. The Macroscopic Traffic Flow Model Equations

We use the method of moments to derive macroscopic equations from the kinetic equations above. To this end, we multiply the inhomogeneous kinetic equation (3) by v^k, $k=0,1$ and integrating it with respect to v in the range of $[0, v_{max}]$ to get the following set of balance equations ;

$$\partial_t\int_0^{v_{max}} v^k f_\alpha(x,v,t)\,dv + \partial_x\int_0^{v_{max}} v^{k+1} f_\alpha(x,v,t)\,dv =$$

$$\int_0^{v_{max}} v^k\{\left(G_B^+ - L_B^+\right)\left(f_{\alpha-1},f_\alpha,f_{\alpha+1}\right) + \left(G_A^+ - L_A^+\right)f_\alpha$$

$$+\left[G_R^+\left(f_\alpha,f_{\alpha+1},f_{\alpha+2}\right) - L_R^+\left(f_\alpha,f_{\alpha+1}\right)\right]$$

$$+\left[G_L^+\left(f_{\alpha-1},f_\alpha\right) - L_L^+\left(f_{\alpha-1},f_\alpha,f_{\alpha+1}\right)\right]\}dv \tag{12}$$

Considering the Gain and Loss terms interactions due to lane changing, acceleration and braking and applying the Dirac delta (δ) function in the sense of distribution, Kimathi [10], we combine equations (6) and (7) to get:

$$\int_0^{v_{max}} v^k\left[G_L^+\left(f_{\alpha-1},f_\alpha\right) - L_L^+\left(f_{\alpha-1},f_\alpha,f_{\alpha+1}\right)\right]dv$$

$$= \left[\rho_{\alpha-1} u_{\alpha-1}^{k} |u_{\alpha-1} - u_{\alpha-1}^{+}| P_R\left(u_{\alpha-1}, \rho_\alpha\right) q_B\left(H_B\left(u_{\alpha-1}\right), \rho_{\alpha-1}\right)\right]$$

$$-\rho_\alpha u_\alpha^{k} |u_\alpha - u_\alpha^{-}| P_L\left(u_\alpha, \rho_{\alpha-1}\right)\left(1 - P_R\left(u_\alpha^{-}, \rho_{\alpha+1}\right)\right) q_B\left(H_B(u_\alpha^{-}), \rho_\alpha\right) \tag{13}$$

similarly equations (4) and (5) give:

$$\int_0^{v_{max}} v^k \left[G_R^{+}\left(f_\alpha, f_{\alpha+1}, f_{\alpha+2}\right) - L_R^{+}\left(f_\alpha, f_{\alpha+1}\right)\right] dv$$

$$= \rho_{\alpha+1} u_{\alpha+1}^{k} |u_{\alpha+1} - u_{\alpha+1}^{-}| P_L\left(u_{\alpha+1}, \rho_\alpha\right)\left[1 - P_R\left(u_{\alpha+1}^{-}, \rho_{\alpha+2}\right)\right] q_B\left(H_B(u_{\alpha+1}^{-}), \rho_{\alpha+1}\right)$$

$$-\rho_\alpha u_\alpha^{k} |u_\alpha - u_\alpha^{+}| P_R\left(u_\alpha, \rho_{\alpha+1}\right) q_B\left(H_B\left(u_\alpha\right), \rho_\alpha\right) \tag{14}$$

Combining equations (8) and (9), we get;

$$\int_0^{v_{max}} v^k \left(G_A^{+} - L_A^{+}\right) f_\alpha \, dv$$

$$\simeq \rho_\alpha h_A q_A\left(H_A\left(u_\alpha\right), \rho_\alpha\right) \frac{\eta - 1}{2} u_\alpha \partial_x u_\alpha \tag{15}$$

similarly equations (10) and (11) give:

$$\int_0^{v_{max}} v^k \left(G_B^{+} - L_B^{+}\right)\left(f_{\alpha-1}, f_\alpha, f_{\alpha+1}\right) dv$$

$$\simeq \rho_\alpha h_B P_B\left(u_\alpha, u_\alpha^{+}, \rho_{\alpha-1}, \rho_{\alpha+1}\right) q_B\left(H_B\left(u_\alpha\right), \rho_\alpha\right) \frac{1 - \beta}{2} u_\alpha \partial_x u_\alpha \tag{16}$$

For equations (15) and (16), we assume that the leading vehicles are distributed in such a way that;

$$h_B q_B\left(H_B(u_\alpha), \rho_\alpha\right) = h_A q_A\left(H_A(u_\alpha), \rho_\alpha\right) = \frac{db\left(\rho_\alpha\right)}{d\rho_\alpha} \tag{17}$$

with $b\left(\rho_\alpha\right)$ being some increasing function of density ρ_α, Kimathi [10]. Therefore the anticipation term is deduced from (15) and (16) using (17), and is written as;

$$a\left(\rho_\alpha, u_\alpha\right) = \begin{cases} \rho_\alpha \dfrac{db\left(\rho_\alpha\right)}{d\rho_\alpha} \varphi_B\left(u_\alpha, u_\alpha^{+}, \rho_{\alpha-1}, \rho_{\alpha+1}\right), & \partial_x u_\alpha < 0 \\ \rho_\alpha \dfrac{db\left(\rho_\alpha\right)}{d\rho_\alpha} \varphi_A\left(u_\alpha\right), & \partial_x u_\alpha > 0 \end{cases} \tag{18}$$

where $\varphi_A\left(u_\alpha\right) = \dfrac{(\eta - 1)}{2} u_\alpha$ and $\varphi_B\left(u_\alpha, u_\alpha^{+}, \rho_{\alpha-1}, \rho_{\alpha+1}\right) = P_B\left(u_\alpha, u_\alpha^{+}, \rho_{\alpha-1}, \rho_{\alpha+1}\right)\left(\dfrac{1 - \beta}{2}\right) u_\alpha$ Assuming that for $\partial_x u_\alpha < 0$, braking is inevitable i.e. $P_B\left(u_\alpha, u_\alpha^{+}, \rho_{\alpha-1}, \rho_{\alpha+1}\right)$ approaches one and taking $\dfrac{(\eta - 1)}{2} u_\alpha \simeq C$, then;

$$a\left(\rho_\alpha\right) = \rho_\alpha \frac{db\left(\rho_\alpha\right)}{d\rho_\alpha} C \tag{19}$$

Using the following specifications of probabilities approximation,

$$P_Y\left(u_\alpha, \rho_\alpha\right) \sim exp\left(-\rho_\alpha \phi\left(u_\alpha\right)\right) = e^{-\rho_\alpha \phi(u_\alpha)}$$

$$q_X\left(H_B\left(u_\alpha\right), \rho_\alpha\right) \sim \frac{1}{1 - \rho_\alpha}$$

and taking $\phi\left(u_\alpha\right) \sim C_0$, the right hand side of equation (13) becomes; for k=0,1:

$$\Phi_1^0\left(\alpha - 1, \alpha, \alpha + 1\right)$$

$$= \rho_{\alpha-1} |u_{\alpha-1} - u_{\alpha-1}^{+}| e^{-\rho_\alpha C_0}\left(\frac{1}{1 - \rho_{\alpha-1}}\right)$$

$$-\rho_\alpha|u_\alpha - u_\alpha^-|e^{-\rho_{\alpha-1}C_0}\left(1-e^{-\rho_{\alpha+1}C_0}\right)\left(\frac{1}{1-\rho_\alpha}\right) \tag{20}$$

$$\Phi_1^1(\alpha-1,\alpha,\alpha+1)$$

$$=\rho_{\alpha-1}u_{\alpha-1}|u_{\alpha-1}-u_{\alpha-1}^+|e^{-\rho_\alpha C_0}\left(\frac{1}{1-\rho_{\alpha-1}}\right)$$

$$-\rho_\alpha u_\alpha|u_\alpha - u_\alpha^-|e^{-\rho_{\alpha-1}C_0}\left(1-e^{-\rho_{\alpha+1}C_0}\right)\left(\frac{1}{1-\rho_\alpha}\right) \tag{21}$$

Similarly for $k=0,1$ the right hand side of equation (14) becomes:

$$\Phi_2^0(\alpha,\alpha+1,\alpha+2)$$

$$=\rho_{\alpha+1}|u_{\alpha+1}-u_{\alpha+1}^-|e^{-\rho_\alpha C_0}\left(\frac{1}{1-\rho_{\alpha+1}}\right)$$

$$\times\left(1-e^{-\rho_{\alpha+2}C_0}\right)-\rho_\alpha|u_\alpha-u_\alpha^+|e^{-\rho_{\alpha+1}C_0}\left(\frac{1}{1-\rho_\alpha}\right) \tag{22}$$

$$\Phi_2^1(\alpha,\alpha+1,\alpha+2)$$

$$=\rho_{\alpha+1}u_{\alpha+1}|u_{\alpha+1}-u_{\alpha+1}^-|e^{-\rho_\alpha C_0}\left(\frac{1}{1-\rho_{\alpha+1}}\right)$$

$$\times\left(1-e^{-\rho_{\alpha+2}C_0}\right)-\rho_\alpha u_\alpha|u_\alpha-u_\alpha^+|e^{-\rho_{\alpha+1}C_0}\left(\frac{1}{1-\rho_\alpha}\right) \tag{23}$$

Taking $f_\alpha(x,v,t)=\rho_\alpha\delta u_\alpha(v)$, then the left hand side of equation (12) becomes:

$$\partial_t\int_0^{v_{max}} v^k\rho_\alpha\delta u_\alpha(v)\,dv+\partial_x\int_0^{v_{max}} v^{k+1}\rho_\alpha\delta u_\alpha(v)\,dv$$

Thus for $k=0$, then:

$$\partial_t\rho_\alpha+\partial_x(\rho_\alpha u_\alpha)=\Phi_1^0(\alpha-1,\alpha,\alpha+1)+\Phi_2^0(\alpha,\alpha+1,\alpha+2) \tag{24}$$

and for $k=1$,

$$\partial_t(\rho_\alpha u_\alpha)+\partial_x(\rho_\alpha u_\alpha^2)-a\left(\rho_\alpha\right)\partial_x u_\alpha$$

$$=\Phi_1^1(\alpha-1,\alpha,\alpha+1)+\Phi_2^1(\alpha,\alpha+1,\alpha+2) \tag{25}$$

Where $a\left(\rho_\alpha\right)$ is the anticipation term from drivers due to speed adaptation effect.
Equations (24) and (25) are the derived macroscopic traffic flow model of Aw-Rascle type.

2.3. The Relaxation Term

In order to reproduce the traffic breakdown that occurs at the bottlenecks such as off and on-ramps, according to the empirical studies done by Kerner [1], we introduce a relaxation term to the velocity dynamics equation (25) as specified in Kimathi [10]. It is through this relaxation term that Kerner's hypothesis of 3-phase traffic flow can also be incorporated into our model for multi-lane traffic flow. The relaxation term $R\left(\rho_\alpha,u_\alpha\right)$ considered for this study is specified as follows:

$$R\left(\rho_\alpha,u_\alpha\right)=\frac{1}{T}\left(U_\alpha^e\left(\rho_\alpha,u_\alpha\right)-u_\alpha\right) \tag{26}$$

where

$$U_\alpha^e\left(\rho_\alpha,u_\alpha\right)=\begin{cases} u_1^e\left(\rho_\alpha\right), & \rho_\alpha<\rho_{\alpha,min}^{syn},\ \ or\ \ u_\alpha>R(\rho_\alpha),\ \ \rho_{\alpha,min}^{syn}<\rho_\alpha<\rho_{\alpha,max}^{free} \\ u_2^e\left(\rho_\alpha\right), & u_\alpha<R(\rho_\alpha),\ \ \rho_{\alpha,min}^{syn}<\rho_\alpha<\rho_{\alpha,max}^{free},\ \ or\ \ \rho_\alpha>\rho_{\alpha,max}^{free}\end{cases} \tag{27}$$

$u_1^e\left(\rho_\alpha\right)$ and $u_2^e\left(\rho_\alpha\right)$ are two optimal velocity curves defined in Kimathi [10] such that $u_2^e\left(\rho_\alpha\right)<u_1^e\left(\rho_\alpha\right)$, $0\le\rho_\alpha<\rho_{\alpha,max}$ with $u_1\left(\rho_{\alpha,max}\right)=u_2\left(\rho_{\alpha,max}\right)=0$ and are monotone decreasing functions of density satisfying the property; $u_1^e\left(\rho_\alpha\right)>R\left(\rho_\alpha\right)>u_2^e\left(\rho_\alpha\right)$, $\rho_{\alpha,min}^{syn}<\rho_\alpha<\rho_{\alpha,max}^{free}$
with $u_2^e\left(\rho_{\alpha,min}^{syn}\right)=R\left(\rho_{\alpha,min}^{syn}\right)$, $u_1^e\left(\rho_{\alpha,max}^{free}\right)=R\left(\rho_{\alpha,max}^{free}\right)$. Here $\rho_{\alpha,min}^{syn}$ is the minimum density below which synchronized flow cannot occur, $\rho_{\alpha,max}^{free}$ is the limit density for free flow existence and $R(\rho_\alpha)$ is a switching curve viewing the traffic dynamics from the density perspective. The curve $u_1^e\left(\rho_\alpha\right)$ characterize the fast mode where the traffic is less dense and allow easy lane change and overtaking manoeuvres. The curve $u_2^e\left(\rho_\alpha\right)$ characterize the slower mode, where the traffic is more dense and give a lesser chance of lane change and overtaking manoeuvres. Therefore equation (25) is written as;

$$\partial_t(\rho_\alpha u_\alpha)+\partial_x(\rho_\alpha u_\alpha^2)-a\left(\rho_\alpha\right)\partial_x u_\alpha=\rho_\alpha R\left(\rho_\alpha,u_\alpha\right)+\Phi_1^1(\alpha-1,\alpha,\alpha+1)+\Phi_2^1(\alpha,\alpha+1,\alpha+2) \tag{28}$$

3. Numerical simulations

For our traffic simulations, we consider a highway with three lanes and an off-ramp as shown in the following Fig. 2 below. For a proper numerical approximation, equations (24) and (28) can be cast into:

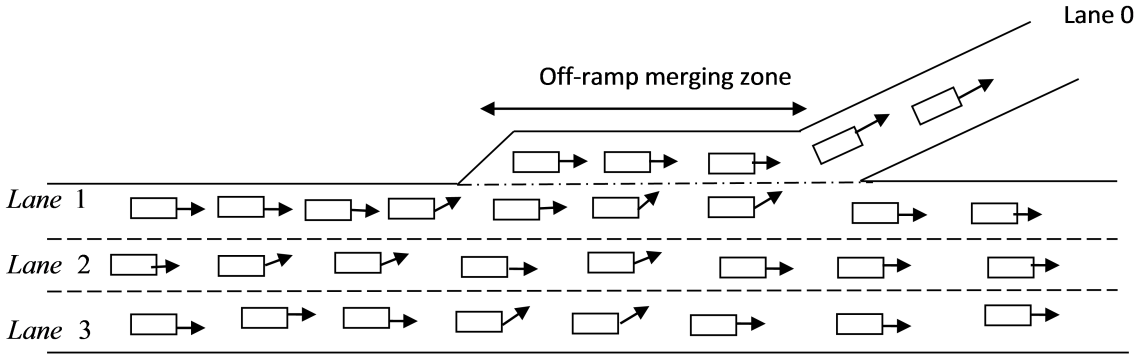

Fig. 2. Section of the highway with three lanes and an off-ramp.

$$\partial_t U_\alpha + \partial_x F(U_\alpha) = S(U_\alpha) \tag{29}$$

Where $U_\alpha = \left(\rho_\alpha, \rho_\alpha u_\alpha + \rho_\alpha p\left(\rho_\alpha\right)\right)^T$, $F(U_\alpha) = \left(\rho_\alpha u_\alpha, \rho_\alpha u_\alpha\left(u_\alpha + p\left(\rho_\alpha\right)\right)\right)^T$ and $S(U_\alpha) = \left(\rho_\alpha u_\alpha, \rho_\alpha u_\alpha\left(u_\alpha + p\left(\rho_\alpha\right)\right)\right)^T$ are vectors of conserved variables, fluxes and the source term respectively.
Given that the general initial data for the homogeneous system of equation below

$$\partial_t U_\alpha + \partial_x F(U_\alpha) = 0 \tag{30}$$

is $\widetilde{U}_\alpha(x, t^n)$, we evolve the solution to a time step $t^{n+1} = t^n + \triangle t$ by use of the Godunov method in the following steps:

- At first we assume a piecewise constant distribution of data by defining cell averages as;

$$U^n_{\alpha,i} = \frac{1}{\triangle x}\int_{x-\frac{1}{2}}^{x+\frac{1}{2}} \widetilde{U}_\alpha\left(x, t^n\right) dx \tag{31}$$

  Then we discretize the spatial domain into M cells, $C_i = \left[x_{i-\frac{1}{2}}, x_{i+\frac{1}{2}}\right]$ for $i = 1....M$ of the same size $\triangle x$. These cell averages produce the required piecewise constant distribution $U_\alpha(x, t^n) = U^n_{\alpha,i}$ data now consist of the set of values $\left\{U^n_{\alpha,i}\right\}$.

- For the rectangular control volume $\left[x_{i-\frac{1}{2}}, x_{i+\frac{1}{2}}\right] \times \left[t^n, t^{n+1}\right]$ shown below in Fig. 3,

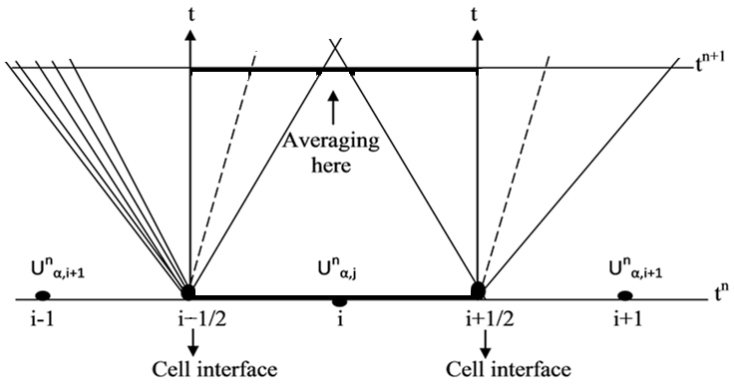

Fig. 3. Typical rectangular control volume.

we obtain the required Godunov numerical scheme as:

$$U_{\alpha,i}^{n+1} = U_{\alpha,i}^{n} + \frac{\triangle t}{\triangle x}\left[F(U_{\alpha,i-\frac{1}{2}}^{n}(0)) - F(U_{\alpha,i+\frac{1}{2}}^{n}(0))\right] \tag{32}$$

Remark 3.1.
In order to contain the interactions of the waves within the cell C_i during the calculations, we impose the Courant-Friedrichs-Lewy restriction ($CFL\ \ condition$) on time step size $\triangle t$ as;

$$\triangle t \leq \frac{C_{cfl}\triangle x}{Max\{\,|\lambda_i(U_\alpha)|,\ \ i=1,2\,\}} \tag{33}$$

where $C_{cfl} \leq 1$, a constant called the Courant number.

This is a condition for numerical stability where a numerical solution is unstable if the errors grow exponentially, which in turn may lead to oscillation of traffic variables with very short wavelength.

To proceed with simulation of our traffic flow features, we introduce the source term $S(U_\alpha)$ to the right hand side of the conservative system of equation (30). The following approximations are used to obtain the equations below; $u_\alpha^+(x,t) \simeq u_\alpha(i+1,k)$ and $u_\alpha^-(x,t) \simeq u_\alpha(i-1,k)$

• For lane 1, i.e when $\alpha = 1$, equations (20) ,(21) ,(22) and (23) respectively becomes;

$$\Phi_1^0(0,1,2) \simeq -\rho_1(i,k)\,|u_1(i,k) - u_1(i-1,k)|\,e^{-\rho_0(i,k)C_0}\left(\frac{1}{1-\rho_1(i,k)}\right)\left(1-e^{-\rho_2(i,k)c_0}\right) \tag{34}$$

$$\Phi_1^1(0,1,2) \simeq -\rho_1(i,k)\,u_1(i,k)\,|u_1(i,k) - u_1(i-1,k)|\,e^{-\rho_0(i,k)C_0}\left(\frac{1}{1-\rho_1(i,k)}\right)\left(1-e^{-\rho_2(i,k)c_0}\right) \tag{35}$$

$$\Phi_2^0(1,2,3) \simeq \rho_2(i,k)\,|u_2(i,k) - u_2(i-1,k)|\,e^{-\rho_1(i,k)C_0}\left(\frac{1}{1-\rho_2(i,k)}\right)$$

$$\times\left(1-e^{-\rho_3(i,k)C_0}\right) - \rho_1(i,k)\,|u_1(i,k) - u_1(i+1,k)|\,e^{-\rho_2(i,k)C_0}\left(\frac{1}{1-\rho_1(i,k)}\right) \tag{36}$$

$$\Phi_2^1(1,2,3) \simeq \rho_2(i,k)\,u_2(i,k)\,|u_2(i,k) - u_2(i-1,k)|\,e^{-\rho_1(i,k)C_0}\left(\frac{1}{1-\rho_2(i,k)}\right)$$

$$\times\left(1-e^{-\rho_3(i,k)C_0}\right) - \rho_1(i,k)\,u_1(i,k)\,|u_1(i,k) - u_1(i+1,k)|\,e^{-\rho_2(i,k)C_0}\left(\frac{1}{1-\rho_1(i,k)}\right) \tag{37}$$

• For lane 2, i.e when $\alpha = 2$, equations (20) ,(21), (22) and (23) respectively becomes;

$$\Phi_1^0(1,2,3) \simeq \rho_1(i,k)\,|u_1(i,k) - u_1(i+1,k)|\,e^{-\rho_2(i,k)C_0}\left(\frac{1}{1-\rho_1(i,k)}\right)$$

$$-\rho_2(i,k)\,|u_2(i,k) - u_2(i-1,k)|\,e^{-\rho_1(i,k)C_0}\left(1-e^{-\rho_3(i,k)C_0}\right)\left(\frac{1}{1-\rho_2(i,k)}\right) \tag{38}$$

$$\Phi_1^1(1,2,3) \simeq \rho_1(i,k)\,u_1(i,k)\,|u_1(i,k) - u_1(i+1,k)|\,e^{-\rho_2(i,k)C_0}\left(\frac{1}{1-\rho_1(i,k)}\right)$$

$$-\rho_2(i,k)\,u_2(i,k)\,|u_2(i,k) - u_2(i-1,k)|\,e^{-\rho_1(i,k)C_0}\left(1-e^{-\rho_3(i,k)C_0}\right)\left(\frac{1}{1-\rho_2(i,k)}\right) \tag{39}$$

$$\Phi_2^0(2,3,4) \simeq \rho_3(i,k)\,|u_3(i,k) - u_3(i+1,k)|\,e^{-\rho_2(i,k)C_0}\left(\frac{1}{1-\rho_3(i,k)}\right)$$

$$-\rho_2(i,k)\,|u_2(i,k) - u_2(i-1,k)|\,e^{-\rho_3(i,k)C_0}\left(\frac{1}{1-\rho_2(i,k)}\right) \tag{40}$$

$$\Phi_2^1(2,3,4) \simeq \rho_3(i,k)\, u_3(i,k)\, |u_3(i,k) - u_3(i+1,k)|\, e^{-\rho_2(i,k)C_0} \left(\frac{1}{1-\rho_3(i,k)}\right)$$

$$-\rho_2(i,k)\, u_2(i,k)\, |u_2(i,k) - u_2(i-1,k)|\, e^{-\rho_3(i,k)C_0} \left(\frac{1}{1-\rho_2(i,k)}\right) \tag{41}$$

• For lane 3, i.e when $\alpha = 3$, equations (22) and (23) vanish since lange-change to lane 4 is not possible. Thus equestions (20) and (21) respectively becomes;

$$\Phi_1^0(2,3,4) \simeq \rho_2(i,k)\, |u_2(i,k) - u_2(i+1,k)|\, e^{-\rho_3(i,k)C_0} \left(\frac{1}{1-\rho_2(i,k)}\right)$$

$$-\rho_3(i,k)\, |u_3(i,k) - u_3(i-1,k)|\, e^{-\rho_2(i,k)C_0} \left(\frac{1}{1-\rho_3(i,k)}\right) \tag{42}$$

$$\Phi_1^1(2,3,4) \simeq \rho_2(i,k)\, u_2(i,k)\, |u_2(i,k) - u_2(i+1,k)|\, e^{-\rho_3(i,k)C_0} \left(\frac{1}{1-\rho_2(i,k)}\right)$$

$$-\rho_3(i,k)\, u_3(i,k)\, |u_3(i,k) - u_3(i-1,k)|\, e^{-\rho_2(i,k)C_0} \left(\frac{1}{1-\rho_3(i,k)}\right) \tag{43}$$

4. Results and discussion

Let the highway under consideration be along the x-axis; where $x = -30$ is the distance upstream of the bottleneck, $x = 0$ is the location of the bottleneck and $x = 10$ is the distance downstream of the bottleneck. Let the flow of traffic be in the direction of increasing x along the axis and $t \in [0, 500]$ be the time interval of the traffic simulation. Simulations of the observed features of spatiotemporal congested traffic patterns that occur in the vicinity of the off-ramp are as shown in Figs. 4 and 5. The various congested traffic patterns of synchronized flow in the upstream and downstream of the off-ramp are also shown in the figures above. It is observed that when the distance to the beginning of the off-ramp merging zone decreases, more vehicles tend to move in lane 1 showing that many vehicles aiming to exit through the off-ramp try indeed to move in lane 2 and 3 as long as possible before changing to lane 1. Thus, when vehicles on lane 1 approach the off-ramp, they decelerate and perform mandatory lane-change if their target is to exit the highway otherwise discretionary lane-change to the right lanes is conducted. That is, on lane 1 a wide moving jam (M) appears upstream of the off-ramp due to the vehicles which change lanes from lane 2 and 3 to lane 1 aiming to exit the highway through the off-ramp. Therefore, traffic congestion is initially set on lane 1 upstream of the beginning of the off-ramp but later this disturbance affect the traffic free flow in lane 2 and 3 near the bottleneck. This happens frequently during rush hours causing heavy traffic to build up on lane 1 upstream of the off-ramp. Hence a stop-and-go traffic pattern is formed near the off-ramp due to vehicles braking as they enter the deceleration lane as depicted in Fig. 4(a). Due to the traffic disturbance caused by the off-ramp inflow rate (q_{in}) and some vehicles in lane 1 going through the highway change lane to lanes 2 and 3, there is an increase in vehicle density and a decrease in vehicle velocity in the three lanes upstream of the bottleneck, Figs. 4 and 5. Fig. 4 (b and c) shows that there is a tendency towards synchronization of vehicles speeds on the highway upstream of the bottleneck indicated by region of fluctuating average low velocities caused by lane changing behavior. In lane 2 and 3, a moving synchronized pattern (MSP) appears on the highway upstream of the off-ramp. Thus lane 1 experiences traffic congestion upstream of the bottleneck where the traffic queue grow at the tail while the vehicles at the head of the queue exit through the off-ramp as shown in Figs. 4 and 5. However, in the three lanes downstream of the off-ramp, there is an immediate decrease in both velocity and density showing that few vehicles are able to manoeuvre out of the traffic merging region. Therefore, there is free flow downstream of the off-ramp after the merging zone in the three lanes where the vehicles have to over-accelerate for the drivers to move at their own desired speed again.

Table 1. Model parameters used in simulations

Parameters	Values	Parameters	Values
$C = c_0$	0.45	$\rho_{\alpha,min}^{syn}$	0.5
C_{cfl}	0.5	$\rho_{\alpha,max}^{free}$	0.3
$\rho_{\alpha,jam}$	0.9		

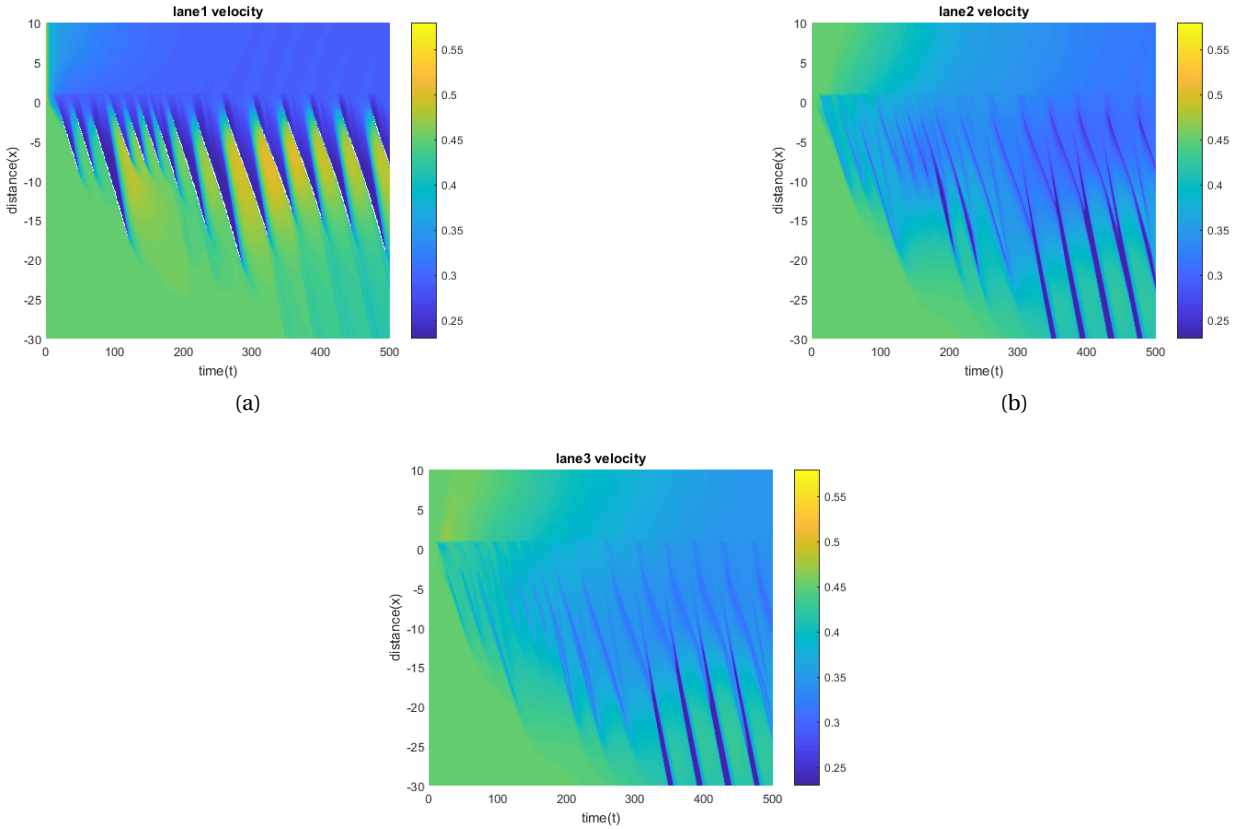

Fig. 4. Velocity space - time traffic patterns of the lanes 1, 2 and 3 near the off-ramp.

Figs. 6, 7 and 8 shows the traffic flow-density relationship in the three lanes, where in lane 1 there is a decrease in flow rate within the deterministic disturbance as the vehicle density increases at the off-ramp ($x = 0$) . It is observed that congestion in lane 1 occurs when the vehicles in lane 2 and 3 change lanes at the beginning of the off-ramp merging zone aiming to exit the highway through the off-ramp. Consequently, the aggressive drivers in lane 1 going through the highway opt to change lanes to the faster ones immediately they approach the traffic merging region. The flow rate in lanes 2 and 3 is sustained at the bottleneck ($x = 0$), see Figs. 7 and 8. This implies that at the bottleneck, most vehicles on the highway prefer to move in lanes 2 and 3 than in lane 1 as long as possible to avoid the vehicles diverging from the highway to the off-ramp. At location ($x = -10$) upstream of the bottleneck, there is a random fluctuation in flow rate with increase of traffic density as shown in Figs. 6, 7 and 8, thus maximum flow rate is attained at low density and vice versa. This traffic flow situation is short lived since vehicles are interacting by changing lanes continuously in the vicinity of an off-ramp. Therefore, a transition of free flow to synchronized flow ($F \rightarrow S$) occurs (where the flow rate is high and the average velocity is low). This ($F \rightarrow S$) transition last for only a short period and transition from synchronized to free flow ($S \rightarrow F$) appear. Thus, the traffic phase transition exchange is continuous at this location and complete a traffic hysteresis loop, in which the upper part of the loop represents the vehicle deceleration branch in ($F \rightarrow S$) transition while the lower part of the loop is the acceleration branch associated with ($S \rightarrow F$).

5. Conclusion

A multi-lane macroscopic traffic flow model of Aw-Rascle type within the framework of the 3-phase traffic flow theory of Kerner has been derived. This has been achieved by applying the method of moments on the kinetic traffic flow model where we obtained the kinetic interaction operators (gain and loss terms). For simulation of our traffic congestion, we have considered a highway with three lanes and an off-ramp. Finite volume method (Godunov scheme) was used to compute the numerical solutions for our traffic flow model equations. The discretized form of the source term equations are obtained for the three lanes in highway and solved using Euler's method. With these simulations near an off-ramp, the derived macroscopic traffic flow model is able to reproduce the spatiotemporal features of real traffic flow near the bottleneck. The simulations show that the initial traffic flow turbulence is experienced only in the lane adjacent to the off-ramp due to the merging of vehicles from lane 2 and 3 aiming to exit the highway through the

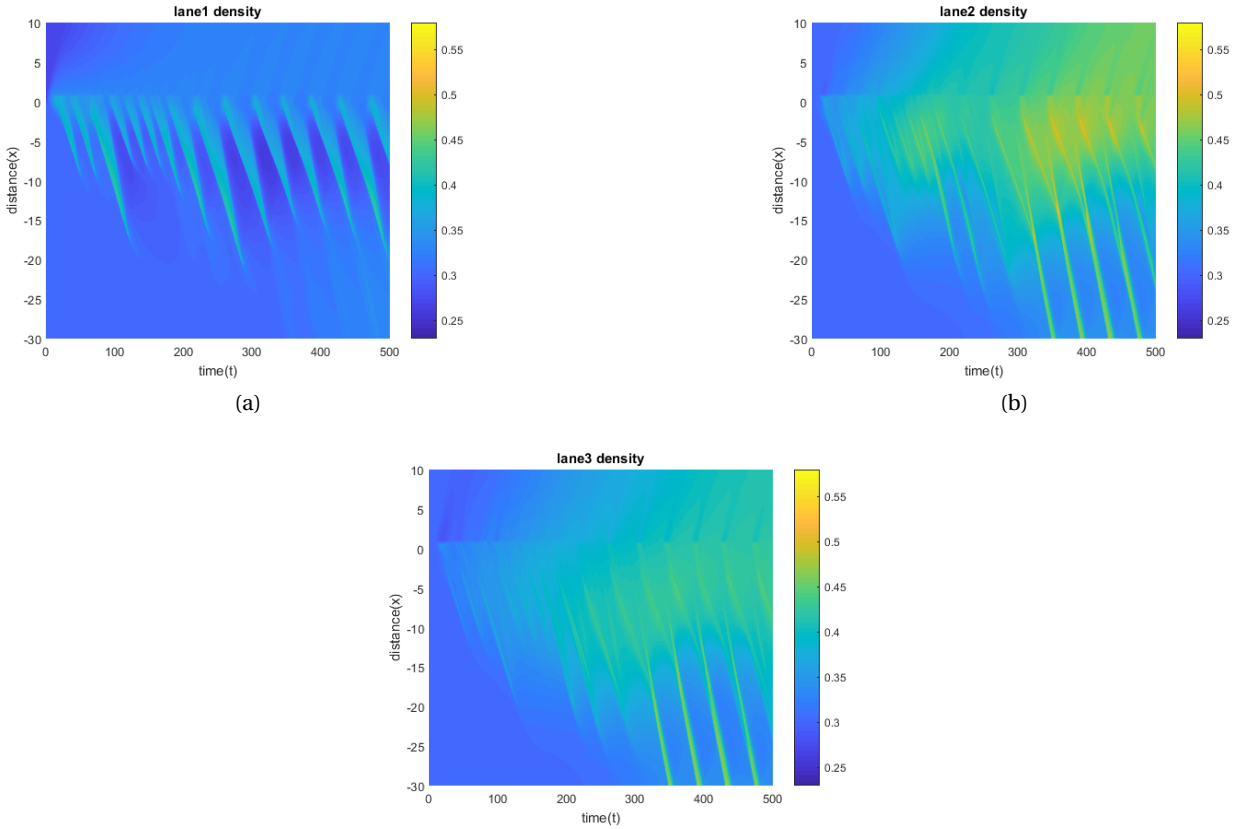

(a) (b) (c)

Fig. 5. Density Space-time traffic patterns of the lanes 1, 2 and 3 near the off-ramp

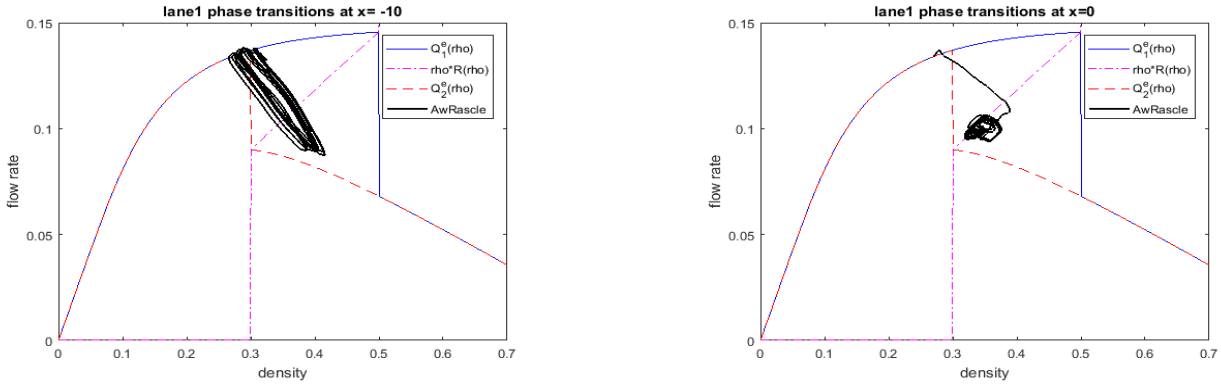

(a) (b)

Fig. 6. Traffic flow rate density relationship in lane 1 at location x is -10 and x is 0

off-ramp. However the disturbance can grow leading to a transition from a free flow to synchronized one, in particular when the vehicle lane-changes leads to the deceleration of the following vehicles in the target lanes and may disrupt the whole traffic near the off-ramp. Therefore vehicles lane-change manoeuvre in the vicinity of an off-ramp can lead to traffic breakdown and congestion. This study shows that the macroscopic multi-lane traffic flow model derived above can be used to;

- improve the design and driveway management in off-ramp areas by identifying the effective location of the bottlenecks to evaluate the impact of new road infrastructure
- solve road congestion problems by either erecting traffic control lights or use the traffic marshals / policemen to control the traffic jam in the vicinity of the highway bottlenecks

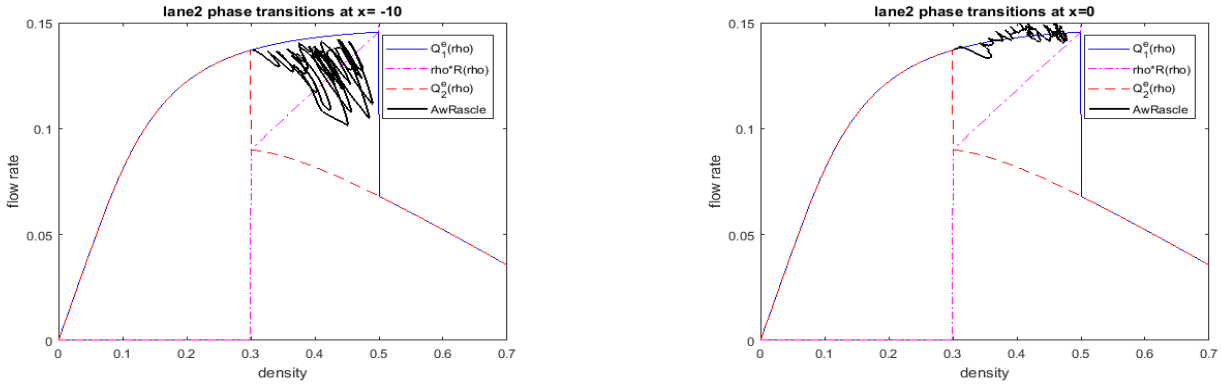

(a) (b)

Fig. 7. Traffic flow rate density relationship in lane 2 at location x is -10 and x is 0

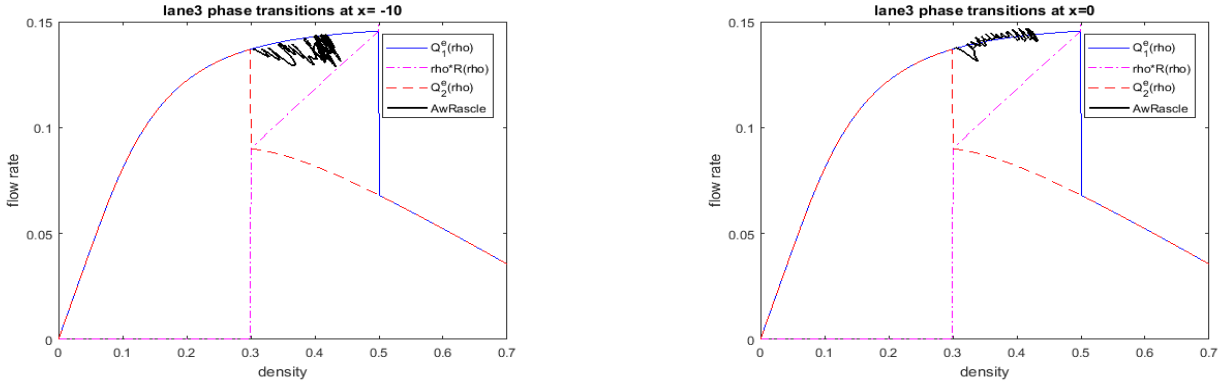

(a) (b)

Fig. 8. Traffic flow rate density relationship in lane 3 at location x is -10 and x is 0

- explain and predict when the traffic jams will emerge at the highway bottlenecks

Recommendations

In this paper, a macroscopic traffic flow model has been derived with traffic simulations done in the vicinity of an off-ramp bottleneck. We recommend that further simulations of traffic congestion near and within weaving section of a highway to be carried out, and a comparison of these results with those of an on and off-ramp be done.

Acknowledgements

I would like to thank my wife Catherine for moral and financial support.

References

[1] B.S Kerner, Introduction to Modern Traffic Flow Theory and Control, The long road to three-phase traffic theory, Springer, first edition, 2009.
[2] G. Whitman, Linear and Nonlinear Waves. Wiley, New York, 1974.
[3] H. Payne, Freflo, A Macroscopic Simulation Model of Freeway Traffic, Transportation Research Record 722 (1979) 68-75.

[4] C. F. Daganzo, Requiem for Second Order Fluid Approximations of Traffic Flow, Transportation Research B29 (4)(1995) 227-286.
[5] A. Aw, M. Rascle, Resurrection of "Second Order" Models of Traffic Flow, SIAM Journal on Applied Mathematics 60(5) (2000) 916-938.
[6] A. Klar, R. Wegener, A Hierarchy of Models for Multilane Vehicular Traffic modeling, SIAM Journal on Applied Mathematics 59(4) (1998) 983-1001.
[7] K. I. Ahmed, Modeling Driver's Acceleration and Lane Changing Behavior, PhD Thesis, Massachusetts Institute of Technology, USA, 1999.
[8] S. P. Hoogendoorn, Multiclass Continuum Modeling of Multilane Traffic Flow, PhD Thesis, Delft University of Technology, Netherlands, 1999.
[9] D. Helbing, A. F. Johansson, On the Controversy Around Daganzo's Requiem for and Aw-Rascle's Resurrection of Second-Order Traffic Flow Models, European Physical Journal B 69(4) (2009) 549-56.
[10] E. M. Kimathi, Mathematical Models for 3-phase Traffic Flow Theory, PhD Thesis, Technical University of Kaiserslautern, Germany, 2012.
[11] M. Amin, J. Banks, Variation in Freeway Lane Use Patterns with Volume, Time of Day, and Location. Journal of the Transportation Research Board 1934: pp 132-139. 2005
[12] Kondli, Elefteriadon, Driver Behavior at Freeway-Ramp Merging Areas Based on Instrumented Vehicle Observations, Transportation Letters 4(3) (2012) 129-142.
[13] C. H. Wei, Developing Freeway Lane-changing Support System using Artificial Neural Networks, *Journal of Advanced Transportation* 35(1) (2001) 47-65.